

Low temperature chemical vapor deposition growth of β -SiC on (100) Si using methylsilane and device characteristics

C. W. Liu^{a)}

Department of Electrical Engineering, National Taiwan University, Taipei 106, Taiwan

J. C. Sturm

Department of Electrical Engineering, Princeton University, Princeton, New Jersey 08544

(Received 7 February 1997; accepted for publication 29 July 1997)

The growth properties of β -SiC on (100) Si grown by rapid thermal chemical vapor deposition, using a single precursor (methylsilane) without an initial surface carbonization step, were investigated. An optimum growth temperature at 800 °C was found to grow single crystalline materials. A simple Al Schottky barrier fabricated on *n*-type SiC grown on Si substrates exhibited a “hard” reverse breakdown of 13 V with a positive temperature coefficient of $2 \times 10^{-4} \text{ }^{\circ}\text{C}^{-1}$ up to 120 °C, indicating an avalanche mechanism. A Pt Schottky barrier fabricated on *n*-type SiC grown on tilted Si substrates to improve the surface morphology exhibited a breakdown voltage of 59 V, with a negative temperature coefficient. From the analysis of the electrical field distribution, the breakdown probably occurred at interface defects between SiC and Si, as suggested by Raman spectroscopy. To investigate minority transport behavior, SiC/Si heterojunction bipolar transistors (HBTs) were fabricated and compared to Si bipolar junction transistors. The collector currents of the SiC/Si HBTs were similar to those of Si control transistors, because both devices had the same base structures. Compared to Si control transistors, the base currents of SiC/Si HBTs increased. It seems that the interface defects between Si and SiC act as recombination centers to deplete back-injected holes, instead of being the barrier to stop hole currents, and thus to increase the base currents of SiC/Si HBTs. © 1997 American Institute of Physics. [S0021-8979(97)03921-2]

I. INTRODUCTION

The unique thermal and electronic properties of SiC make it a promising material for electronic and optoelectronic devices designed to operate in extreme conditions such as high voltage, high temperature, high frequency, and high radiation. SiC has many different one-dimensional polytypes (different stacking sequences). A repetitive ABC stacking sequence yields a zincblende structure, referred to as 3C or β -SiC. The other about 170 non-cubic crystals are referred to as the α -SiC family. Recently, most of the research activities and progress have been made on α -SiC, primarily 6H and 4H,^{1,2} because of the mature bulk crystal technologies.³ There are no suitable substrates of β -SiC crystals, but β -SiC epilayer has been grown in the past on Si (100) substrates, despite a 20% mismatch of lattice constants and an 8% mismatch of thermal expansion coefficients between β -SiC and Si. Conventionally, the chemical vapor deposition growth of β -SiC on Si requires high growth temperatures ($\geq 1300 \text{ }^{\circ}\text{C}$)⁴ using separate precursors such as SiH₄ for Si and C₃H₈ for C, and an initial high temperature surface carbonization step,^{5,6} which prevents the possibility of integration with silicon-based devices. Furthermore, the low material quality is reflected in very leaky Schottky barriers with the highest reported soft breakdown of only 8–10 V.⁷ In this study, we report growth properties of cubic SiC on (100) Si grown at temperature as low as 700 °C using a single gas precursor “methylsilane” without the carbonization step, first demonstrated by Golecki *et al.*⁸ We describe the material properties of the films using x-ray diffraction,

Raman scattering, Fourier transform infrared absorption, and transmission electron microscope, and then discuss Schottky barriers and Si/SiC heterojunction bipolar transistors fabricated on these films.

II. GROWTH

Due to the lack of suitable β -SiC substrates, β -SiC was grown on Si (100) substrates. The SiC films were deposited on tilted (4° towards ⟨110⟩) and nontilted Si substrates (within 1° off) with a diameter of 100 mm by rapid thermal chemical vapor deposition (RTCVD) at a growth temperature of 700–1100 °C. The growth pressure was 1 Torr with a 1.5 sccm methylsilane (SiCH₆) flow and a 500 sccm hydrogen flow. The growth temperature (700–800 °C) was accurately determined by the infrared transmission technique.⁹ Growth temperatures higher than 800 °C were controlled by the tungsten-halogen lamp power which was previously calibrated with a thermocouple welded onto a Si wafer. The SiC thickness was measured by fitting the optical reflection spectra from 500 to 700 nm with the SiC index of refraction of 2.6. Since the temperature is not uniform across the wafer (the edge is about 50 °C lower than the center), the thickness was measured at the spot very close to the position where the temperature was monitored (near the center of the wafer). Figure 1 gives the Arrhenius plot of the growth rate of SiC on nontilted (100) Si. The growth rate in the range 700–800 °C varied exponentially with the inverse of temperature and the activation energy for this surface-reaction-limited growth was 3.6 eV. This is higher than that of pure silicon growth using silane as a precursor (~1.7 eV)¹⁰ and may reflect the strong C–H bonding energy. At a higher growth

^{a)}Electronic mail: chee@cc.ee.ntu.edu.tw

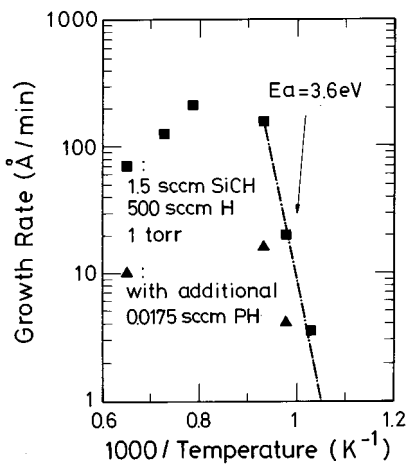


FIG. 1. Arrhenius plot of the growth rate of SiC on nontilted (100) Si. Note that the phosphorus incorporation decreases the growth rate.

temperature (800–1100 °C), the growth rate had a weak temperature dependence, indicating mass-transport-limited growth.

The crystallinity of the films was studied by x-ray diffraction (XRD) and transmission electron microscope (TEM). For the films grown at 750 °C, the XRD spectrum [Fig. 2(a)] of an 80 nm film on nontilted substrates exhibited a single crystalline feature with a broad unresolved Cu $K_{\alpha 1}$ and Cu $K_{\alpha 2}$ (400) peak [full width half maximum (FWHM) of 2θ is about 1.6°]. But the TEM diffraction pattern [Fig. 2(b)] of the same sample showed evidence of some slightly in-plane rotated textures and very fine spots in the ⟨110⟩ direction. This indicates the poor crystallinity of the 750 °C films. The crystallinity can be improved by increasing the growth temperature to 800 °C. The XRD spectrum [Fig. 3(a)] of a 0.23 μm SiC film grown at 800 °C on nontilted substrates showed that the FWHM of unresolved Cu K_{α} (400) peak was as small as 0.75°, which was similar to the value (0.65–0.7°) of 0.3 μm commercial (100) SiC on Si,⁸ which was grown at a much higher temperature (≥ 1300 °C). The TEM diffraction pattern [Fig. 3(b)] also displayed a well-defined single crystalline feature. The films grown at 800 °C on tilted substrates had similar XRD spectra and TEM diffraction patterns, but had relatively smoother surface morphologies, compared to nontilted substrates, as observed under the optical microscope. This facilitated the Schottky barrier fabrication on tilted substrates to reduce leakage current. TEM also showed very high densities of stacking faults and dislocations, similar to films of similar thickness grown by conventional high temperature growth techniques. The Fourier transform infrared (FTIR, not shown here) spectra of a 0.23 μm 800 °C grown film on nontilted substrates displayed an absorption peak at 796 cm⁻¹ (TO phonon absorption) with a FWHM of 50 cm⁻¹, which is similar to that of the film grown by conventional high temperature growth methods.¹¹ The Raman spectrum (Fig. 4) of the same sample showed a broad peak at 960 cm⁻¹ with FWHM of 60 cm⁻¹ and a sharp peak 510 cm⁻¹. The 510 cm⁻¹ peak is associated with the Si substrates, not SiC epilayers. The peak near 960 cm⁻¹ is probably due to a com-

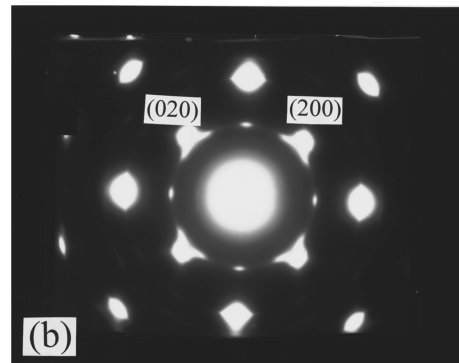
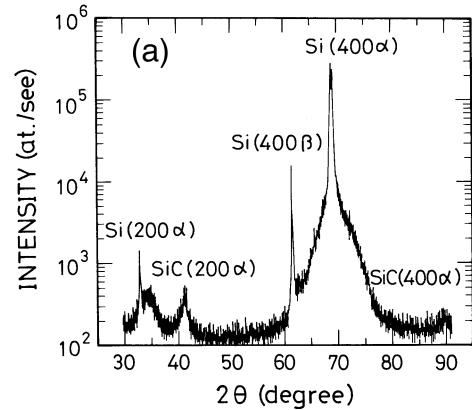


FIG. 2. The XRD spectrum (a) and TEM diffraction pattern (b) of a 750 °C-grown film with a thickness of 80 nm.

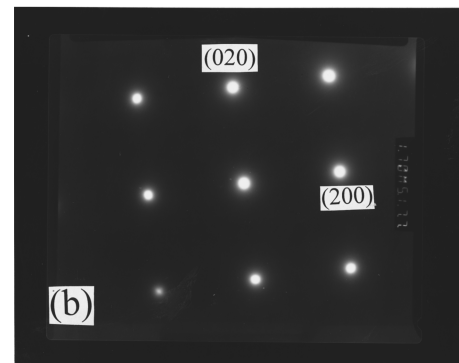
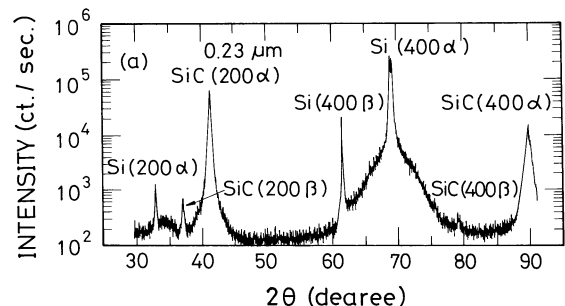


FIG. 3. The XRD spectrum (a) and TEM diffraction pattern (b) of a 800 °C-grown film with a thickness of 0.23 μm.

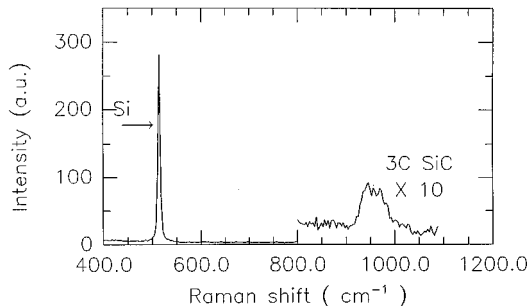


FIG. 4. The Raman spectrum of a $0.23\text{ }\mu\text{m}$ $800\text{ }^{\circ}\text{C}$ grown film.

bination of the LO phonon scattering ($\sim 970\text{ cm}^{-1}$) and interface defects between SiC and Si.¹² The XRD spectrum of the film grown at 1000 and $1100\text{ }^{\circ}\text{C}$, however, reveals extra (111) and (220) peaks, indicating the growth of polycrystalline material. Therefore, the $800\text{ }^{\circ}\text{C}$ is the optimum growth temperature for the single crystalline β -SiC. However, “two step growth,” namely, a thin layer grown at $800\text{ }^{\circ}\text{C}$ first, followed by high temperature growth, can improve the single crystallinity of the films. For example, a film with a thickness of $0.45\text{ }\mu\text{m}$ grown at $1000\text{ }^{\circ}\text{C}$ formed a polycrystalline structure [Fig. 5(a)] However, if a $0.15\text{ }\mu\text{m}$ layer was deposited at $800\text{ }^{\circ}\text{C}$, followed by a $0.3\text{ }\mu\text{m}$ film grown at $1000\text{ }^{\circ}\text{C}$, this improved the single crystalline quality of the layers grown at $1000\text{ }^{\circ}\text{C}$ [Fig. 5(b)]. This shows that a low growth temperature ($800\text{ }^{\circ}\text{C}$) at the SiC/Si interface is essential for the growth of single crystalline layers by this technique, in contrast to what is often observed in conventional growth techniques which require high growth temperatures and surface carbonization at the SiC/Si interface to improve crystallinity.

III. DOPING

Unintentionally doped β -SiC layers always show *n*-type conduction.¹³ Although there was some controversy initially,

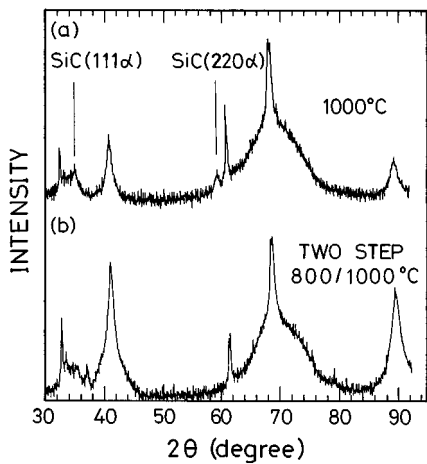


FIG. 5. The XRD spectra of a $1000\text{ }^{\circ}\text{C}$ grown film with a thickness of $0.45\text{ }\mu\text{m}$ (a) and a “two-step” film (b). A $0.15\text{ }\mu\text{m}$ layer was deposited at $800\text{ }^{\circ}\text{C}$ first, then followed by a $0.3\text{ }\mu\text{m}$ layer grown at $1000\text{ }^{\circ}\text{C}$ for the “two-step” film.

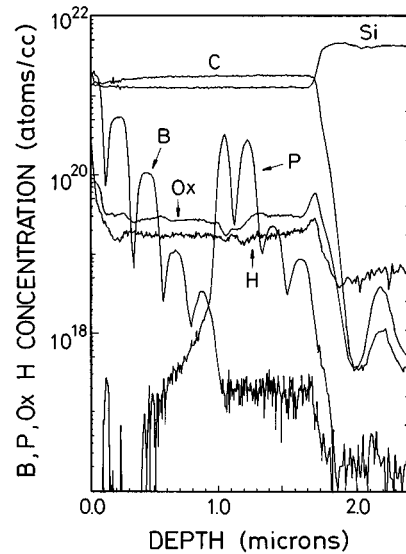


FIG. 6. A SIMS plot of SiC multilayers with impurity incorporations. The growth temperature was $800\text{ }^{\circ}\text{C}$ except the top layer. The bumps are the doped layers with different phosphine (or diborane) flows. The valleys are the undoped spacers. Note that the top layer was a diborane-doped film grown at $750\text{ }^{\circ}\text{C}$.

there appears to be agreement that the origin of the *n*-type conduction is controlled by a shallow donor (nitrogen) with a binding energy of $15\text{--}20\text{ meV}$.¹³ Note that nitrogen source in our growth system is thought to come from the methylsilane gas precursor, which was only 99% pure. Nitrogen was also commonly used as the *n*-type dopant in β -SiC. On the other hand, very limited studies of phosphorus-doped SiC have been reported. The *p*-type dopant of Al is popularly used to obtain *p*-type SiC, because of its relatively low acceptor binding energy of 0.24 eV , compared to boron with the value of 0.735 eV . In this work, we investigate the *in situ* incorporation of boron and phosphorus into β -SiC.

The boron and phosphorus incorporation are accomplished by introducing diborane (10 ppm in hydrogen) and phosphine (70 ppm in hydrogen) precursors, respectively, into gas mixtures. Their incorporation into $800\text{ }^{\circ}\text{C}$ grown β -SiC layers was measured by secondary-ion mass spectroscopy [SIMS, (Fig. 6)] on a multilayer sample with various dopant gas flows. Each doped layer was grown for 10 min and separated by unintentionally doped spacers grown for 5 min. We did not perform systematic study of the residual dopant effect on the undoped spacers, but the undoped spacers seemed to work well to separate the adjacent doped layers. For SiGe layers grown in the same chamber, the turn-off slope of phosphorus doping in the doped SiGe was about 300 \AA/decade from 3×10^{18} to 10^{17} cm^{-3} . Both boron and phosphorus showed approximately linear incorporation with the gas flow up to the concentrations of 5×10^{20} and $3 \times 10^{20}\text{ cm}^{-3}$ for boron and phosphorus, respectively (Fig. 7, compiled from SIMS data). No systematic Hall measurements or direct electrical activation measurements versus dopant level was performed. The SIMS data also indicated that there were large amounts of oxygen and hydrogen contamination in our SiC films grown at $800\text{ }^{\circ}\text{C}$ with the concentrations of

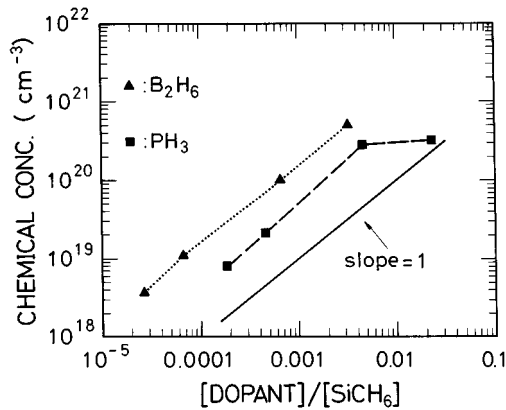


FIG. 7. The chemical concentrations of dopant (P and B) in SiC as a function of ratio of actual dopant flow to methylsilane flow at a growth temperature of 800 °C.

3×10^{19} and $2 \times 10^{19} \text{ cm}^{-3}$, respectively. One interesting observation is that phosphorus incorporation with high phosphine to methylsilane flow ratio ($\sim 1.2 \times 10^{-2}$, corresponding chemical concentration of $3 \times 10^{20} \text{ cm}^{-3}$) reduced the growth rate of SiC by a factor of 10 and 5 for the growth temperatures of 800 and 750 °C, respectively (Fig. 1). SIMS (Fig. 6) also showed that the width of the highest peak in the P profile with the phosphine to methylsilane flow ratio of 3×10^{-2} becomes narrower (indicating a slower growth rate) as compared with other phosphorus doped layers with lower phosphine flow rates. A suppressed growth rate due to phosphine incorporation has also been reported in Si epitaxial growth.¹⁴ Boron incorporation can be utilized to compensate the background impurities of the SiC films. This increases the breakdown voltage of Schottky diodes fabricated on SiC films as shown in Sec. IV.

IV. SCHOTTKY BARRIERS

The SiC grown on Si by conventional high temperature techniques has various kinds of defects, which cause very leaky diodes with soft breakdown voltage less than 10 V.⁷ Although the (111) β -SiC grown on 6H SiC has been demonstrated with a hard breakdown voltage of 200 V,¹⁵ the temperature coefficient of breakdown voltage is negative, which is contradictory to the avalanche process. Therefore, we fabricated Schottky barriers on (100) β -SiC grown on Si to study the reverse breakdown characteristics, using this low temperature growth technique. The samples used for Schottky barriers were grown at 800 °C. Since the unintentionally doped SiC films were *n*-type with carrier concentrations around 10^{18} cm^{-3} or higher as determined by Hall measurement, boron compensation was necessary to reduce the net dopant concentration of SiC films. The chemical concentration of boron used for this purpose was about 10^{20} cm^{-3} (measured by SIMS in samples grown under similar conditions). However, most boron might be located in non-electrically active interstitial sites.¹⁶ The electrically active acceptor concentration is estimated about 1% of the chemical concentration.¹⁷ Therefore, the active acceptor concentration was the same order of magnitude of the background donor

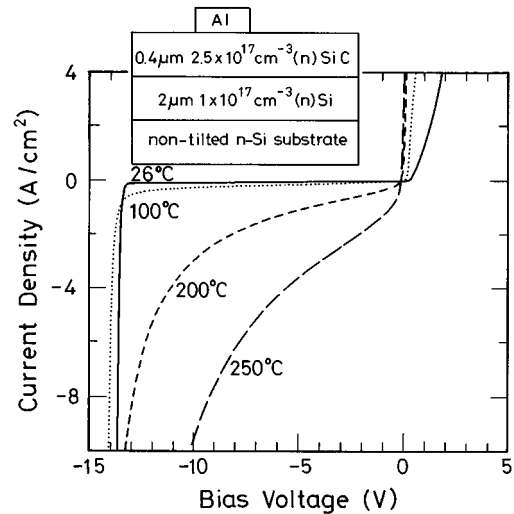


FIG. 8. The *I*-*V* characteristics of Al Schottky barriers. The insert is the device structure. A positive temperature coefficient was observed for the reverse breakdown voltage.

concentration. To get the least amount of net dopant concentration in the SiC layers, sometimes we grew a series of films with different B_2H_6 flows, and then picked the best diodes fabricated from those films. Before metal evaporation, the boron-compensated *n*-type SiC films were cleaned in dilute HF without any extra polishing, oxidation, and etching.⁷ The size of Schottky barriers was defined either by photolithography or by shadow masks. Two kinds of Schottky barrier structures were studied:

(a) Al (500 nm) Schottky barriers of size $1.3 \times 10^{-4} \text{ cm}^2$ were fabricated on $0.4 \mu\text{m}$, $2.5 \times 10^{17} \text{ cm}^{-3}$ *n*-type SiC, with a $2 \mu\text{m}$, $1 \times 10^{17} \text{ cm}^{-3}$, *n*-type Si buffer on nontilted Si (100) *n*-type substrates as shown in the insert of Fig. 8.

(b) Pt (80 nm) Schottky barriers of size $1.3 \times 10^{-3} \text{ cm}^2$ were fabricated on $1 \mu\text{m}$, $1 \times 10^{16} \text{ cm}^{-3}$, *n*-type SiC with $4 \mu\text{m}$, $1 \times 10^{17} \text{ cm}^{-3}$, *n*-type Si buffers, but on tilted *p*-type substrates as shown in the insert of Fig. 9.

Because of the rough morphology of thick layers ($> 0.5 \mu\text{m}$) grown on non-tilted substrates, the structure (b) was grown on tilted substrates (4° toward $\langle 110 \rangle$) to get a smooth morphology, which reduced the leakage current of the Schottky diodes. The Al was deposited by a thermal evaporator. The Pt evaporation was performed by an electron beam evaporator. Instead of being held at elevated temperature,¹⁸ our samples were not intentionally heated during Pt evaporation. The net dopant concentrations of SiC were measured by capacitance-voltage (*C*-*V*) measurement after the Schottky barriers were made.

The diodes were measured by current-voltage (*I*-*V*) and high frequency *C*-*V* at 1 MHz in a light-tight box. One probe made contact to the Schottky barrier itself and the other to a large metal contact away from the barrier. Since both contacts are on the same side of the wafer, the diodes have large series resistance, which has serious effect on forward *I*-*V* characteristics in terms of ideality factors. We therefore only focused on the reverse breakdown behaviors and made comparison to previous results. The reverse *I*-*V*

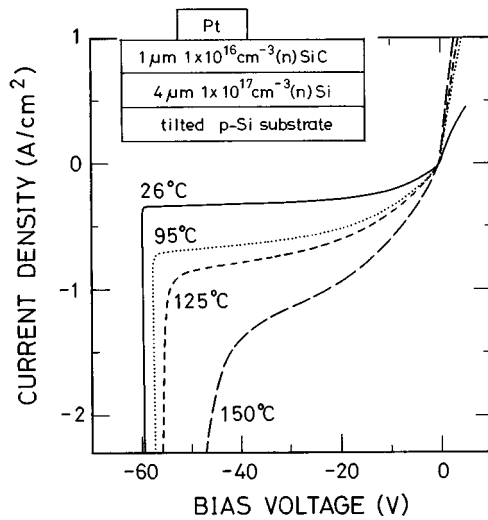


FIG. 9. The I - V characteristics of Pt Schottky barriers. The insert is the device structure.

characteristics of the Al Schottky barriers [structure (a)] had a hard breakdown voltage of 13 V (Fig. 8). To avoid the effect of reverse leakage current, the value of breakdown voltage is obtained by extrapolating the current at breakdown to the x axis (voltage axis). The depletion depth at the breakdown was about 0.22 μm obtained from the C - V measurement (Fig. 10), and was completely confined in the SiC layer. The breakdown electric field calculated from breakdown voltage and doping concentration was 1×10^6 V/cm, about one third of the theoretical value for β -SiC.¹⁹ The reduction compared to the ideal value is possibly due to the defects of the SiC lattice using this growth method. The temperature coefficient of breakdown voltage showed a positive value of about $2 \times 10^{-4} \text{ }^\circ\text{C}^{-1}$ from room temperature to 120 $^\circ\text{C}$, and became negative above 190 $^\circ\text{C}$ with soft breakdown. Unlike the previous reported negative value¹⁵ for Schottky barriers on β -SiC heteroepitaxially grown on 6H SiC, this is the first observation of a positive temperature coefficient of breakdown voltage in β or α -SiC grown by any method. Such a positive temperature coefficient is highly desirable in device applications to prevent runaway if devices reach the breakdown point. This also indicates that

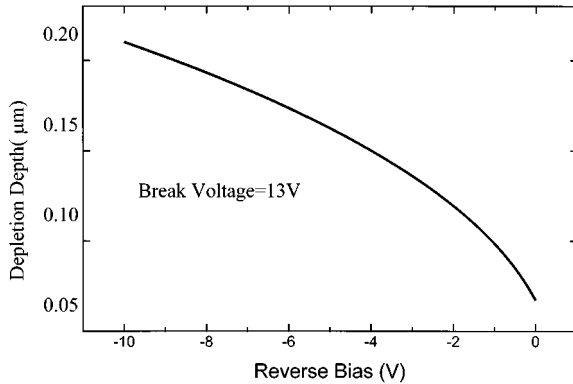


FIG. 10. The depletion depth as a function of reverse bias voltage for an Al Schottky barrier. The depletion depth at breakdown was about 0.22 μm .

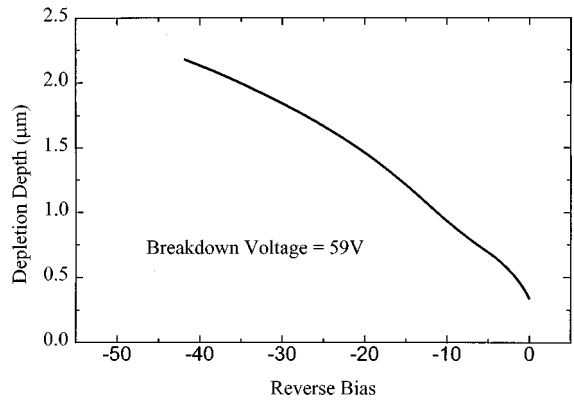


FIG. 11. The depletion depth as a function of reverse bias voltage for a Pt Schottky barrier. The depletion depth at breakdown was about 2.5 μm and terminated in the n -type Si layer.

impact ionization avalanche transit time (IMPATT) diodes can possibly be made in β -SiC, because the positive temperature coefficient is the direct result of an impact ionization process,²⁰ required for the IMPATT diodes. Combined with the high electron saturation velocity (two times of Si value), the IMPATT diodes based on the β -SiC material might reach an oscillation frequency of 200 GHz. The Al Schottky barriers showed the same I - V characteristics after annealing at 500 $^\circ\text{C}$ for 10 min in a forming gas without any degradation.

The reverse I - V characteristics of Pt Schottky barriers in Fig. 9 showed 59 V breakdown voltage, and the depletion depth at breakdown was 2.5 μm obtained from C - V measurement (Fig. 11), implying that the entire SiC layer (1 μm) was depleted and the depletion region terminated in the n -type Si layer. The electric field in SiC and Si, calculated from Poisson's equation and doping profile obtained from C - V , did not reach the breakdown field of either SiC (1×10^6 V/cm) or Si ($\sim 6 \times 10^5$ V/cm). The breakdown probably occurred at the interface defects between SiC and Si due to the misfit of lattice constants and thermal expansion coefficients, the presence of which were suggested by Raman spectroscopy. Recently, there was a report that the oxygen in the gas mixture also formed voids at the SiC/Si interface.²¹ The defects and voids between the SiC and Si interface probably lowers the breakdown electrical field of the avalanche process. Note that since the breakdown voltage (59 V) is much larger than the $6E_g/q$ (E_g is the band gap, 2.2 eV, and q is the electron charge), the breakdown is an avalanche process.²⁰ The temperature coefficient of breakdown voltage had a negative value of $4 \times 10^{-4} \text{ }^\circ\text{C}^{-1}$ from room temperature to 120 $^\circ\text{C}$. The Pt Schottky barriers degraded after forming gas annealing at 500 $^\circ\text{C}$ for 10 min, showing a soft breakdown around 10 V. This is contrary to the results of Ref. 18, where the Pt Schottky barriers showed improved reverse I - V characteristics at a reverse bias of a few volts after isochronal annealing. This controversy may be ascribed to the breakdown in the Si/SiC interface of our Schottky barriers, instead of in the bulk SiC. The breakdown voltage should be improved by using the n^+ -SiC layer below the active SiC layer to terminate all the electric field lines

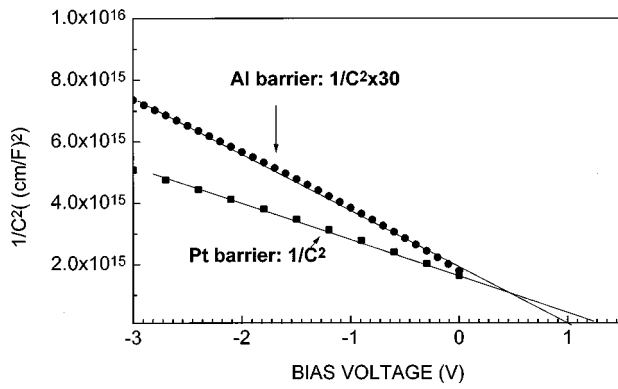


FIG. 12. The $1/C^2$ vs bias voltage plots for Pt and Al Schottky contacts on β -SiC.

before the field lines reach the interface. Please note that the reverse saturation currents of Al and Pt barriers are 6×10^{-2} and 0.3 A/cm^2 , respectively, which are much higher than the β -SiC pn diodes grown on 6H SiC in Ref. 15, but the origin is not clear.

The barrier heights of both barriers can be obtain from the expression:

$$\Phi_b = V_i + \zeta - \Delta\Phi + kT/q,$$

where V_i is the intercept of $1/C^2$ vs V plots (Fig. 12), ζ is the difference between conduction-band edge and Fermi level, $\Delta\Phi$ is the image force lowering, and kT/q is the thermal voltage. Using the ζ and $\Delta\Phi$ values in Ref. 18, the barrier heights of Pt and Al barriers are 1.4 eV and 1.1 eV, respectively. The Pt barrier height agrees well with the previous reported value (1.35 eV),¹⁸ while a higher value (1.69 eV) was reported on (n11) orientation.¹⁶ The barrier height of Al barriers, which were deposited in an ultrahigh-vacuum chamber, was estimated as 1.4 eV by the photoemission method.²²

V. HETEROJUNCTION BIPOLAR TRANSISTORS

Despite the success with Si/SiGe/Si HBTs, there is still a strong desire for a wide gap emitter material on Si. Such a wide gap emitter on a Si base could yield devices with better high temperature performance than Si/SiGe HBTs (due to higher band gap) and might be easier to be integrated.²³ The high current gain in a wide band gap emitter HBT may be also traded for low base resistance. This low base resistance, combined with a short base transit time in a very thin base, will produce transistors of high speed performance compatible with existing polysilicon-emitter technologies. Several materials such as semi-insulating polycrystalline Si (SIPOS), amorphous Si, GaP, and β -SiC have been reported to serve this purpose.²⁴ A current gain of 800 has been obtained by β -SiC grown by a special technique at 1000 °C on (111) Si substrates.²⁵ However, the high temperature process of 1000 °C would produce excessive back diffusion and prevent the integration with other Si devices. The band gap of β -SiC is 2.2 eV, but the band alignment between β -SiC and Si is not known.

Si BJT

$n^+(10^{18}\text{cm}^{-3})$	— Si emitter $\sim 2000 \text{ \AA}$	(800 °C)
$n(10^{17}\text{cm}^{-3})$	— Si emitter $\sim 3000 \text{ \AA}$	(800 °C)
$p^+(10^{19}\text{cm}^{-3})$	— Si base $\sim 600 \text{ \AA}$	(700°C)
$n(10^{17}\text{cm}^{-3})$	— Si collector $\sim 3000 \text{ \AA}$	(800°C)
$n^+(10^{19}\text{cm}^{-3})$	— Si collector $\sim 2\mu\text{m}$	(1000°C)

< 100 > non-tilted n Si substrates

SiC/ Si HBT

$n^+(10^{18}\text{cm}^{-3})$	— Si emitter $\sim 2000 \text{ \AA}$	(800 °C)
$n^+(10^{18}\text{cm}^{-3})$	— SiC emitter $\sim 2000 \text{ \AA}$	(800 °C)
$n(10^{17}\text{cm}^{-3})$	— Si emitter $\sim 3000 \text{ \AA}$	(800 °C)
$p^+(10^{19}\text{cm}^{-3})$	— Si base $\sim 600 \text{ \AA}$	(700°C)
$n(10^{17}\text{cm}^{-3})$	— Si collector $\sim 3000 \text{ \AA}$	(800°C)
$n^+(10^{19}\text{cm}^{-3})$	— Si collector $\sim 2\mu\text{m}$	(1000°C)

< 100 > non-tilted n Si substrates

FIG. 13. Layer structures of a Si bipolar junction transistor and a SiC/Si heterojunction bipolar transistors. There is an additional SiC layer between the n-Si emitter and the n^+ -Si emitter in the SiC/Si HBT.

The single crystalline β -SiC grown at 800 °C on (100) Si substrates was used for the wide band gap emitter material of Si/SiC HBTs. Figure 13 displays the layer structures of a Si control device (Si bipolar junction transistors) and a SiC/Si HBT. In the SiC/Si HBT, there is an additional 2000 Å unintentionally doped SiC layer ($n = 10^{18} \text{ cm}^{-3}$) between the n-Si emitter and the n^+ -Si emitter. Note that the n^+ -Si emitter grown on the SiC layer in the SiC/Si HBT structure was polycrystalline, confirmed by x-ray diffraction. The heavily doped base ($p = 10^{19} \text{ cm}^{-3}$) is designed to increase the maximum frequency of oscillation by reducing the base sheet resistance. To avoid the tunneling current in the emitter junction, a 0.3 μm moderately doped Si emitter ($n = 10^{17} \text{ cm}^{-3}$) was grown, followed by the heavily doped emitter layers.²⁶ The thickness of the n-type Si emitter is small compared to the hole diffusion length, which is estimated to be about 10 μm for hole mobility of 330 cm/V s and life time of 0.1 μs . Therefore, the hole diffusion in the emitter will be affected by the boundary condition at the SiC/Si interface. Note that Si/SiGe/Si HBTs with a record-high maximum frequency of oscillation of 160 GHz have used this structure of a heavily doped base and a moderately doped Si emitter followed by a heavily doped emitter layer.²⁷ Similar doping or structural profiles were used in Refs. 28–30. As a result, the depletion width of the emitter varied from 1100 to 600 Å as the emitter-base voltage varied from 0 to 0.7 V, within the moderately doped Si emitter, while the depletion width in the heavily doped base varied from 110 from 60 Å. However, the interface between SiC and Si is defective due to the 20% misfit, the emitter junction of SiC/Si HBTs is designed in the Si/Si pn junction, instead of the Si/SiC pn junction, to avoid

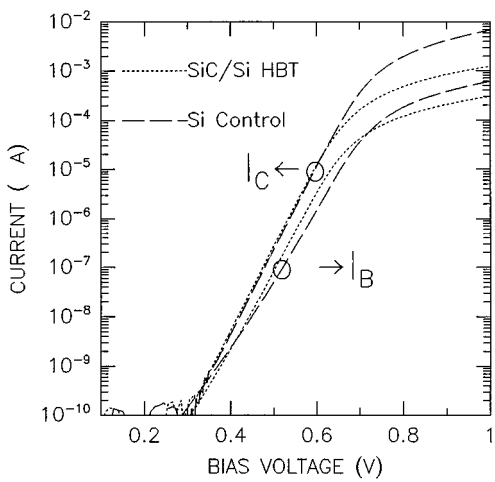


FIG. 14. The Gummel plots of a SiC/Si HBT and a Si control device. The base current of the β -SiC/Si HBT was higher than that of the Si control device, while the collector currents for both devices were very similar due to identical base structures of these two devices.

the recombination current in the depletion region of the emitter junction. There might be two main effects of the SiC layer in the emitter on device performance. The desired one is that the n -SiC layer can block back-injected hole current (base current) as a diffusion barrier and thus increases the current gain. This is similar to poly-Si BJTs.²³ An undesired effect is that the defective SiC/Si interface might act as a recombination center for hole current and thus decrease the current gain. The defect density of Si/SiC interface will determine which effect is larger. The transistors were fabricated using a double-mesa process, which was detailed in Refs. 31 and 32. The base contact was established by boron implant. Before base implantation, the emitter mesas were formed by plasma etching (SF₆ for Si and 8% O₂ in CF₄ for SiC). The devices were isolated by plasma-etched mesas and passivated with SiO₂ deposited by plasma deposition at 350 °C. Before contact metallization, the wafers were given a RCA clean, and annealed at 700 °C for 30 min in a forming gas. The emitter size was 60 $\mu\text{m} \times 60 \mu\text{m}$ for both HBTs and BJTs.

Figure 14 shows the base current and collector current as a function of the emitter-base voltage (Gummel plot). The collector-base voltage is fixed at 2 V. The collector currents for both devices showed same voltage (V_{be}) dependence with an ideality factor of 1.0 and the same absolute magnitude. This result is expected, because both devices have the same base structures and the same barriers for electron transport from the emitter to the collector. The base currents also showed near-ideal behavior with ideality factors of 1.2 and 1.1 for Si BJTs and SiC/Si HBTs, respectively. However, the desired enhancement of current gain (I_c/I_b) was not observed, because the base currents of SiC/Si HBTs was higher than those of Si BJTs. For example, the current gains are 3.7 and 7.7 for HBTs and BJTs, respectively, at the emitter base voltage of 0.6 V. The current gains (I_c/I_b) of both devices are also shown in Fig. 15 and the Si BJT has higher current gain than the SiC/Si HBT at high collector current. The increase of base currents in the SiC/Si HBT's, compared to the

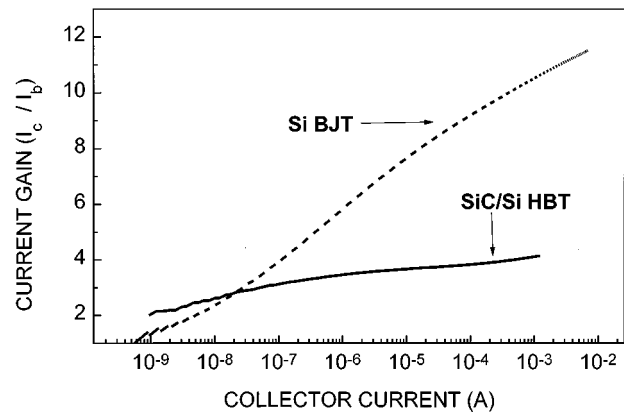


FIG. 15. The current gain vs collector current plots for Si BJTs and SiC/Si HBTs.

Si BJT's, indicated that the interface defects between Si and SiC acted as recombination centers for back-injected holes. Therefore, the back-injected holes recombined at the SiC/Si interface. The wide band gap SiC layer would be a barrier to stop the hole current if the interface defects were removed and there was no recombination hole current at the SiC/Si interface. Moreover, the fact that the base current is dominated by hole diffusion current in the neutral emitter is confirmed by the ideality factor of base currents. If the base hole currents were from the recombination in the depletion region of emitter junction, the ideality factor should be the same for both HBTs and BJTs, since both depletion regions were within the n -type Si emitters. However, a more ideal base current was observed in the HBTs ($n = 1.1$) than in the BJTs ($n = 1.2$). This indicates that the dominant base current occurs in a neutral emitter region in the HBTs and not in a depletion region or a device edge (surface). Note also the apparent high series resistance of the HBTs. This is thought to result from the SiC layer in the emitter. The SiC/Si HBT did not increase the current gain compared to the Si BJT due to the defective interface. To reduce the defect density at the interface, a passivation technology of the interface will be desired in the future.

VI. SUMMARY

A single crystalline β -SiC has been grown at 800 °C on Si. The growth temperature of 800 °C was essential for initial single crystalline SiC layers on Si (100) substrates. Schottky barriers on n -type SiC on (100) Si showed a hard reverse breakdown voltage as high as 59 V. A positive temperature coefficient of breakdown voltage of SiC was observed for the first time with the breakdown voltage of 13 V. The density of interface defects should be further reduced for desired SiC/Si HBT performance.

ACKNOWLEDGMENTS

The TEM assistance of Dr. E.A. Fitzgerald of ATT Bell Labs and Professor P. Pirouz and Dr. J. W. Yang of Case Western Reserve University, and the SIMS analysis of Dr. C. W. Magee of Evan East are gratefully appreciated. The support of the U.S. Office of Naval Research (Grant No.

N000121-90-J-1316) is gratefully acknowledged. One of the authors (C.W.L.) would like to thank the support of the National Science Council of the Republic of China under Contract No. 85-2215-E-005-002 for publishing this article.

- ¹M. Bhatnagar, B. J. Baliga, H. R. Kirk, and G. A. Rozgonyi, IEEE Trans. Electron Devices **43**, 150 (1996).
- ²C. Schroder, W. Heiland, R. Held, and W. Loose, Appl. Phys. Lett. **68**, 1957 (1996).
- ³Y. M. Tairov and V. F. Tsvetkov, J. Cryst. Growth **52**, 146 (1981).
- ⁴P. Liaw and R. F. Davis, J. Electrochem. Soc. **132**, 642 (1985).
- ⁵S. Nishino, Y. Hazuki, H. Matsunami, and T. Tanaka, J. Electrochem. Soc. **127**, 2674 (1980).
- ⁶S. Nishino, J. A. Powell, and H. A. Will, Appl. Phys. Lett. **42**, 460 (1983).
- ⁷D. E. Ioannou, N. A. Papanicolaou, and P. E. Nordquist, IEEE Trans. Electron Devices **34**, 1694 (1987).
- ⁸I. Golecki, F. Reidinger, and J. Marti, Appl. Phys. Lett. **60**, 1703 (1992).
- ⁹J. C. Sturm, P. V. Schwartz, E. J. Prinz, and H. Manoharan, J. Vac. Sci. Technol. B **9**, 2011 (1991).
- ¹⁰J. L. Regolini, D. Bensahel, J. Mercier, and E. Scheid, Appl. Phys. Lett. **54**, 658 (1989).
- ¹¹J. P. Li, J. Steckl, I. Golecki, and F. Reidinger, Appl. Phys. Lett. **62**, 3135 (1993).
- ¹²Z. C. Feng, A. J. Mascarenhas, W. J. Choyke, and P. A. Powell, J. Appl. Phys. **64**, 3176 (1988).
- ¹³J. A. Freitas, S. G. Bishop, P. E. R. Nordquist, and M. L. Gipe, Appl. Phys. Lett. **52**, 1695 (1988).
- ¹⁴M. L. Yu, D. J. Vitkavage, and B. S. Meyerson, J. Appl. Phys. **59**, 4032 (1986).
- ¹⁵P. G. Neudeck, D. J. Larkin, J. E. Star, J. A. Powell, C. S. Salupo, and L. G. Matus, IEEE Electron Device Lett. **14**, 136 (1993).
- ¹⁶R. F. Davis, G. Kelner, M. Shur, J. Palmour, and J. A. Edmond, Proc. IEEE **79**, 677 (1991).
- ¹⁷H. J. Kim and R. F. Davis, J. Electrochem. Soc. **133**, 2350 (1986).
- ¹⁸N. A. Papanicolaou, A. Christou, and M. L. Gipe, J. Appl. Phys. **65**, 3526 (1989).
- ¹⁹M. Bhatnagar and B. J. Baliga, IEEE Trans. Electron Devices **40**, 645 (1993).
- ²⁰S. Sze, *Physics of Semiconductor Devices* (Wiley, New York, 1981), pp. 98 and 566.
- ²¹A. Leycuras, Appl. Phys. Lett. **70**, 1533 (1997).
- ²²V. M. Bermudes, J. Appl. Phys. **63**, 4951 (1988).
- ²³T. K. Ning and D. D. Tang, Proc. IEEE **74**, 1669 (1986).
- ²⁴S. Sze, *High-Speed Semiconductor Devices* (Wiley, New York, 1990), p. 366.
- ²⁵T. Sugii, T. T. Ito, Y. Furumura, M. Doki, F. Mieno, and M. Maeda, IEEE Electron Device Lett. **9**, 87 (1988).
- ²⁶Z. Matutinovic-Krstelj, E. J. Prinz, P. V. Schwartz, and J. C. Sturm, IEEE Electron Device Lett. **12**, 163 (1991).
- ²⁷A. Schuppen, U. Erben, A. Gruhle, H. Kibbel, H. Schumacher, and U. Konig, Tech. Dig. Int. Electron. Device Meet. 743 (1995).
- ²⁸E. J. Prinz, P. M. Garone, P. V. Schwartz, X. Xiao, and J. C. Sturm, IEEE Electron Device Lett. **12**, 42 (1991).
- ²⁹S. S. Lu, C. C. Wu, C. C. Huang, F. Williamson, and M. I. Nathan, Appl. Phys. Lett. **60**, 2138 (1992).
- ³⁰H. R. Chen, C. P. Lee, C. Y. Chang, J. S. Tsang, and K. L. TSai, J. Appl. Phys. **74**, 1398 (1993).
- ³¹L. D. Lanzerotti, A. St. Amour, C. W. Liu, J. C. Sturm, J. K. Watanabe, and N. D. Theodore, IEEE Electron Device Lett. **17**, 334 (1996).
- ³²Z. Matutinovic-Krstelj, V. Venkataraman, E. J. Prinz, and J. C. Sturm, IEEE Trans. Electron Devices **43**, 457 (1996).